Journal of Physics: Conference Series **160** (2009) 012039 doi:10.1088/1742-6596/160/1/012039

Performance of the PAMELA Si-W Imaging Calorimeter in Space

V Bonvicini[1], M Boezio[1], E Mocchiutti[1], A Vacchi[1], G Zampa[1], N Zampa[1], R Bellotti[2], A Bruno[2], F Cafagna[2], O Adriani[3], L Bonechi[3], M Bongi[3], S Bottai[3], D Fedele[3], P Papini[3], S Ricciarini[3], P Spillantini[3], E Taddei[3], E Vannuccini[3], G Castellini[4], M Ricci[5], G A Basilevskaja[6], A N Kvashnin[6], Y I Stozhkov[6], A M Galper[7], L Grishantseva[7], S V Koldashov[7], A Leonov[7], V V Mikhailov[7], S A Voronov[7], Y T Yurkin[7], V G Zverev[7], G Barbarino[8], G De Rosa[8], G Osteria[8], D Campana[8], M Casolino[9], M P De Pascale[9], V Malvezzi[9], L Marcelli[9], M Minori[9], P Picozza[9], R Sparvoli[9], E A Bogomolov[10], S Y Krutkov[10], G Vasilyev[10], W Menn[11], M Simon[11], P Carlson[12], P Hofverberg[12], S Orsi[12], M Pearce[12]

[1]INFN – Sezione di Trieste, Padriciano 99, I-34012 Trieste (Italy)

[2]INFN – Sezione di Bari and Physics Department of University of Bari, Via Amendola 173, I-70126 Bari (Italy)

[3]INFN – Sezione di Firenze and Physics Department of University of Florence, Via Sansone 1, I-50019 Sesto Fiorentino, Florence, Italy

[4]IFAC, Via Madonna del Piano 10, I-50019 Sesto Fiorentino, Florence, Italy

[5]INFN, Laboratori Nazionali di Frascati, Via Enrico Fermi 40, I-00044 Frascati, Italy

[6]Lebedev Physical Institute, Leninsky Prospekt 53, RU-119991 Moscow, Russia

[7]Moscow Engineering and Physics Institute, Kashirskoe Shosse 31, RU-11540 Moscow, Russia

[8]INFN – Sezione di Napoli and Physics Department of University of Naples "Federico II", Via Cintia, I-80126 Naples, Italy

[9]INFN – Sezione di Roma 2 "Tor Vergata" and Physics Department of University of Rome "Tor Vergata", Via della Ricerca Scientifica 1, I-00133 Rome, Italy

[10]Ioffe Physical Technical Institute, Polytekhnicheskaya 26, RU-194021 St. Petersburg, Russia

[11]Physics Department of Universität Siegen, D-57068 Siegen, Germany

[12] KTH, Department of Physics, Albanova University Centre, SE-10691 Stockholm, Sweden

Correspoding author email: bonvicini@ts.infn.it

Abstract. The Payload for Antimatter-Matter Exploration and Light Nuclei Astrophysics (PAMELA), primarily designed to directly measure antiparticles (antiprotons and positrons) in the cosmic radiation, was launched successfully on June 15th, 2006, and, since then, it is in continuous data taking. The calorimeter of the PAMELA apparatus has been designed to identify antiprotons from an electron background and positrons from a background of protons with high efficiency and rejection power. It is a sampling silicon-tungsten imaging calorimeter, which comprises 44 single-sided silicon sensor planes (380 μm thick) interleaved with 22 plates of tungsten absorber (0.74 X_0 each). It is the first silicon-tungsten calorimeter to be launched in space. In this work we present the in-orbit performance of the calorimeter, including the measured identification capabilities. The calorimeter provides a proton rejection factor of ~10^5 while keeping a high efficiency in selecting electrons and positrons, thus fulfilling the identification power needed to reach the primary scientific objectives of PAMELA. We show also that, after almost two years of operation in space, the calorimeter is still performing nominally.

1. Introduction

PAMELA (a Payload for Antimatter Matter Exploration and Light-nuclei Astrophysics) is a satellite-borne experiment designed to study charged particles in the cosmic radiation, with a particular emphasis on antiparticles (antiprotons and positrons). PAMELA is installed inside a pressurized container mounted onboard the Russian Resurs DK-1 earth-observation satellite that was launched into space by a Soyuz-U rocket on June 15th, 2006 from the Baikonur cosmodrome (Kazakhstan) [1]. The satellite orbit is elliptical and quasi-polar, with an inclination of 70.4º and an altitude varying between 350 and 610 km. The minimum estimated lifetime of the mission is 3 years.

The primary scientific goal of the mission is the study of the antimatter component of the cosmic radiation, in order to:

- Search for evidence of dark matter particle annihilations;
- Search for antinuclei (in particular, antihelium);
- Test cosmic-ray propagation models through precise measurements of the antiparticles energy spectra.

Other important scientific goals include: the study of solar physics and solar modulation during the 24th solar minimum, and the study of the cosmic-ray electron energy spectrum up to several TeV, thereby allowing possible contributions from local sources to be identified [1].

Table 1 shows the design goals for PAMELA performance, presenting the cosmic-ray components and energy ranges over which PAMELA will give new results.

Table 1. Design goals for PAMELA performance

Cosmic-ray particle	Energy range
Antiprotons	80 MeV – 190 GeV
Positrons	50 MeV – 270 GeV
Electrons	50 MeV – 400 GeV
Protons	80 MeV – 700 GeV
Electrons + positrons	Up to 2 TeV
Light nuclei (up to Z=6)	100 MeV/n – 200 GeV/n
Antinuclei	Sensitivity 95% CL
Antihelium/Helium ratio	$O(10^{-7})$

2. The PAMELA apparatus

A schematic overview of the PAMELA apparatus is shown in figure 1. The apparatus is ~ 1.3 m high, has a total mass of 470 kg and an average power consumption of 355 W.

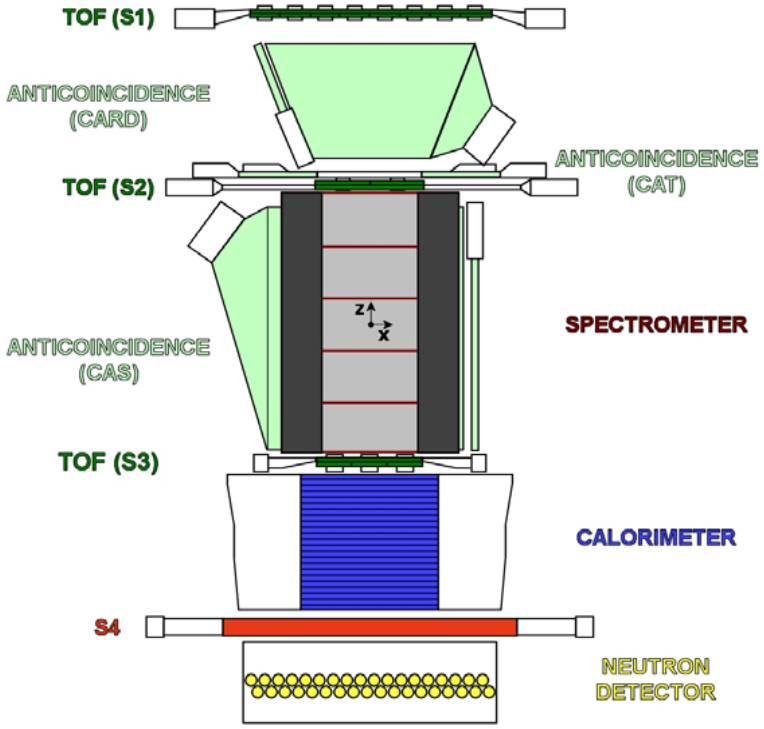

Figure 1. Schematic overview of the PAMELA instrument

The central part of the apparatus is a magnetic spectrometer, consisting of a permanent magnet and a silicon tracker [2]. The magnet provides a uniform magnetic field of 0.43 T along the *y* direction. The dimensions of the cavity of the magnet define the geometrical factor of the experiment to be 21.5 cm^2 sr. The tracking system consists of six planes of double-sided silicon microstrip detectors for precise reconstruction of the particle trajectory. The spectrometer measures the magnetic deflection of charged particles and, consequently, their momentum. The spatial resolution of the tracker in the bending view is observed to be, during flight, ~ 3 μm, which corresponds to a maximum detectable rigidity (MDR) of about 800 GV.

The electromagnetic calorimeter, to which the next sections of this paper are devoted, is installed below the magnetic spectrometer.

The Time-of-Flight (ToF) system of the experiment is based on three double layers of fast plastic scintillators (S1, S2 and S3), with alternate layers placed orthogonally to each other [3]. The ToF system provides a fast signal for triggering the data acquisition in the PAMELA subdetectors, and measures the time of flight and ionization energy losses of traversing particles.

The anticoincidence (AC) system consists of four plastic scintillators (CAS) surrounding the sides of the magnet, one (CAT) covering the top and four (CARD) enclosing the volume between the first two ToF planes [4]. The aim of the AC system is to identify false triggers and multiparticle events, generated by secondary particles produced in the apparatus.

Below the electromagnetic calorimeter, a single square plastic scintillator (S4) acts as a shower-tail catcher and is used to generate a high energy trigger signal for the underlying neutron detector (ND). The purpose of the neutron detector is to complement the electron-proton discrimination capabilities of the calorimeter by detecting the increased neutron production associated with hadronic showers in

the calorimeter compared with electromagnetic ones. It consists of ^{3}He proportional counters surrounded by a polyethylene moderator enveloped by a thin cadmium layer [5].

3. The electromagnetic imaging calorimeter

3.1. Physics tasks of the PAMELA calorimeter

The main task of the calorimeter is to select positrons and antiprotons from the large background constitued by protons and electrons, respectively. Positrons have to be identified from a background of protons that is about 10^3 times the positrons component at 1 GeV/c, increasing to ~ 5 x 10^3 at 10 GeV/c. Antiprotons have to be selected from a background of electrons that decreases from ~ 5 x 10^3 times the antiproton component at 1 GeV/c to less than 10^2 times above 10 GeV/c. This means that PAMELA must be able to separate electrons from hadrons at a level better than 10^5. Much of this rejection power in PAMELA is provided by the calorimeter.

Besides the electron-hadron separation, the calorimeter must also directly measure the energy of electrons and positrons.

3.2. Calorimeter structure

The sampling imaging calorimeter comprises 44 single-sided silicon strip detector planes interleaved with 22 plates of tungsten absorber [6]. Each tungsten layer is 0.74 X_0 thick (2.6 mm) and it is sandwiched between two printed circuit boards, which house the silicon detectors as well as the front-end and digitizing electronics. Each silicon plane consists of 3x3, 380 μm thick, 8x8 cm^2 detectors, segmented into 32 strips with a pitch of 2.4 mm. The orientation of the strips for two consecutive silicon planes is shifted by 90°, thus providing 2-dimensional spatial information. Each of the 32 strips is wire-bonded to the corresponding strip on the other two detectors in the same row (or column), thereby forming 24 cm long readout strips. The total depth of the calorimeter is 16.3 X_0 (~ 0.6 λ_I). The high granularity of the calorimeter and the use of silicon strip detectors provide detailed information on the longitudinal and lateral profiles of particles' interactions as well as a measure of the deposited energy.

Figure 2 shows the calorimeter prior to integration with the other PAMELA detectors. The instrument is ~ 21 cm tall and the sesitive area of the silicon planes is 24 x 24 cm^2.

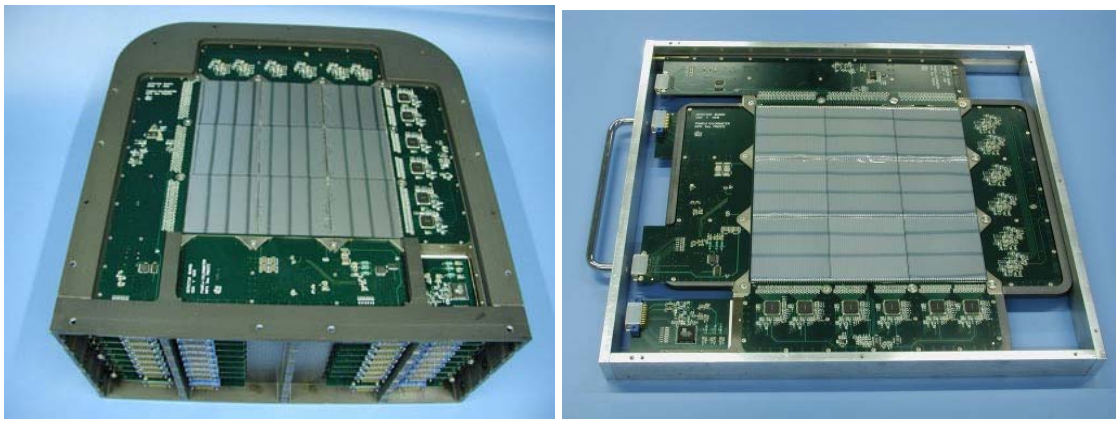

Figure 2. Left: The PAMELA Si-W imaging calorimeter with the topmost silicon plane visible. Right: Detail of a single calorimeter module (formed by 2 tungsten plates and 4 silicon planes) before being inserted into the calorimeter main frame.

3.3. Front-end and data acquisition electronics

The calorimeter front-end electronics is based on the CR1.4P full custom ASIC [7], which provides 16 channels featuring a charge-sensitive preamplifier, a CR-RC shaping amplifier, a track-and-hold

circuit and an output multiplexer. An input-selectable calibration circuit and a self-trigger circuit are also implemented in the chip (see subsection 4.3).

A key feature of the CR1.4P is its wide dynamic range (~ 1400 Minimum Ionizing Particles, or about 7.1 pC for 380 μm thick silicon detectors). The large dynamic range is of crucial importance to correctly measure the interactions of high energy particles inside the calorimeter. Another important characteristics of the CR1.4P is the low noise slope as a function of the detector input capacitance, which allows the circuit to provide a good signal-to-noise ratio for 1-MIP signals (~ 9:1) while coping with the rather large (~ 180 pF) capacitance presented at its input by the 24 cm long calorimeter strips. Table 2 summarizes the main characteristics of the CR1.4P.

Six CR1.4P chips are used to read-out each of the 44 silicon planes (264 chips are used for the whole calorimeter). In each plane, the analog outputs of the front-end chips are multiplexed into a single 16-bit ADC (Analog Devices AD977A).

For redundancy purposes, the read-out is divided into 4 independent sections (exploiting the segmentation of the calorimeter), corresponding to x-even, y-even, x-odd and y-odd planes. Data from all 44 ADCs are processed by 4 read-out boards mounted on the front cover of the calorimeter. Four FPGA (Altera A54SX72), one per section, control all data acquisition and slow control processes and, in normal acquisition mode ("compress mode"), transmit the data to 4 DSPs (Analog Devices ADSP2187), which perform the tasks of first-level data analysis and compression and the calculations associated with the instrument on-line calibration (pedestal, baseline, noise rms, etc.). The calibration is performed once per orbit, at the equator crossing from the southern emisphere. After each calibration a special run is performed, in which both raw (non-compressed) and compressed data are transmitted ("full mode"). In this way it is possible to check the correct functioning of the compression algortihm. The FPGAs also monitor and check the status of the DSPs and, in case of failure of one of them, can bypass the malfunctioning DSP and transmit directly the raw data of that section to the main PAMELA DAQ ("raw mode").

Table 2. Main characteristics of the CR1.4P front-end circuit

Number of channels	16
Supply	±5 V
Total power consumption	97 mW
Max. output swing	7 V
Gain (sensitivity)	5 mV/MIP
Linear dynamic range	1400 MIP (7.1 pC)
Noise@C_{det} = 0 pF	2700 e^- rms
Noise slope	4.7 e^- / pF
Non-linearity	< 1% full range

4. In-flight performance of the calorimeter

After its launch from Baikonur on June 15th 2006, PAMELA was first switched-on on June 20th and, after a brief commissioning phase, the instrument has been in continous data taking mode since July 11th. At the time this paper is being written, more than 10 Tbyte of raw data have been downlinked to Earth and ~ 10^9 triggers have been recorded by PAMELA.

4.1. Basic performance

After two years of operation in space, no failures or loss of functionality have been observed in the calorimeter. All basic parameters (temperatures, pedestals, noise, gain) are stable and nominal.

For example, figure 3 displays the pedestal of one channel measured from May 2006 (i.e. before launch) to June 2007. This stable behaviour is common to all calorimeter channels.

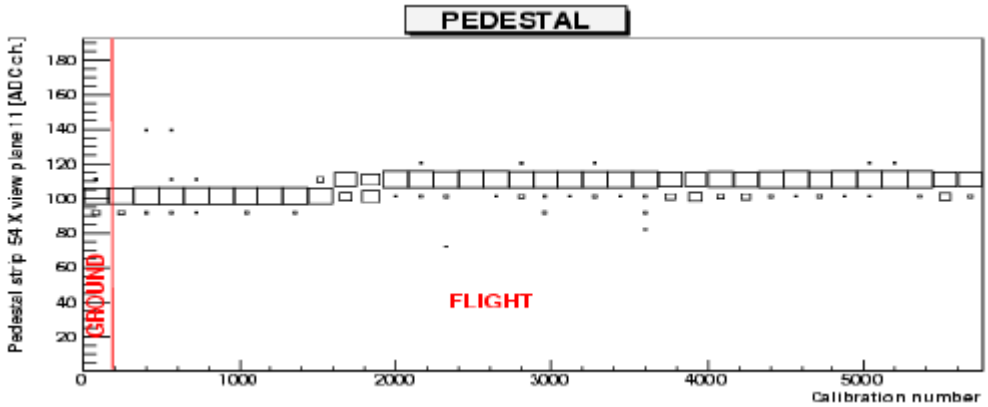

Figure 3. Pedestal of one strip of the calorimeter from May 2006 (prior to PAMELA launch) to July 2007 (one year after the launch) in ADC channels.

Figure 4 (left) shows the rms noise of another calorimeter channel measured in a time period spanning from July 2006 to January 2008, while figure 4 (right) shows, for the same channel and the same period, the position of the peak of the pulse height distribution. The stability in time of these parameters, hence of the signal-to-noise ratio, is clearly seen.

4.2. Physics performance

As mentioned in section 3, the imaging calorimeter of PAMELA has been designed to precisely reconstruct the longitudinal and lateral profiles of interactions and to measure the deposited energy. The longitudinal and lateral segmentation of the calorimeter, combined with the measurement of the particle energy loss in each strip, allows a very high identification (or rejection) power for electromagnetic showers. For example, figure 5 shows a 84 GeV/c antiproton interacting in the calorimeter and giving rise to a typical hadronic shower pattern, while figure 6 shows a 92 GeV/c positron giving an electromagnetic shower in the calorimeter.

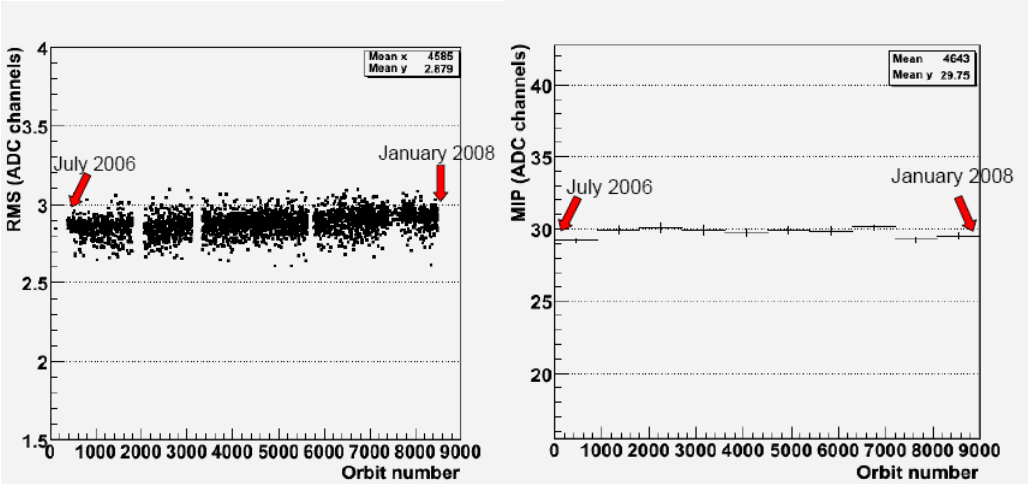

Figure 4. Left: rms noise (in ADC channels) of one calorimeter channel from the start of the mission to January 2008. Right: Peak of the pulse height distribution (in ADC channels) for the same channel and over the same time interval.

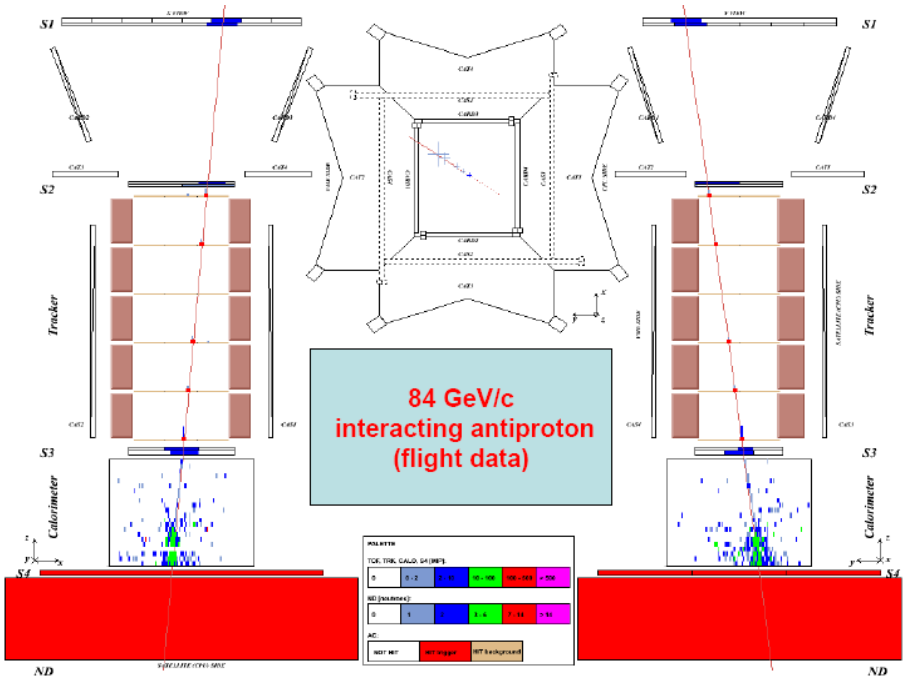

Figure 5. Event display of an interacting 84 GeV/c antiproton from flight data.

The e/h discrimination power of the calorimeter is obviously fundamental for the physics analysis, especially for the extraction of the positron signal from the proton backgound. An example of the calorimeter capabilities in the positron selection is illustrated in figures 7 and 8. Figure 7 shows a sample of flight data (positive and negative, with rigidity between 20 and 30 GV, as selected by the magnetic spectrometer) in which we have plotted the distribution of the ratio between the charge released along the track in the calorimeter (obtained by summing the signal in the hit strip and the signals in the left and right neighboring strips) and the total charge measured in the calorimeter. In these plots, the non-interacting antiprotons and protons are clearly seen, peaked at one. In the negative plot, the distribution due to the electrons is clearly seen (due to the paucity of the antiprotons), while in the positive plot the positron sample (expected to be peaked at an energy fraction corresponding to that of the electrons) is completely overwhelmed by the background of interacting protons. In figure 8 we have imposed several conditions: the request that the energy measured by the calorimeter matches the momentum measured by the magnetic spectrometer ("energy-momentum match") and various topological cuts related to the starting point of the shower and its longitudinal profile: the positron sample is now clearly visible in the data. It should be noted that the cuts mentioned above are just an example for the purpose of showing the calorimeter capabilities in e/h separation. In the positron data analysis, additional topological and energy-related conditions are used.

5. Conclusions

The satellite-borne experiment PAMELA has been studying cosmic rays for two years. Throughout this period, the Si-W imaging calorimeter of the apparatus has been performing nominally. In particular, all functional parameters (temperature, pedestals, noise, signal, gain) are nominal and stable. The physics performance are consistent with the expectations, with the simulations and test beam results. During two years of operation in space, no failures nor loss/degradation of performance have been observed and the calorimeter proved to be able to fulfill the requirements needed to achieve the scientific goals of PAMELA.

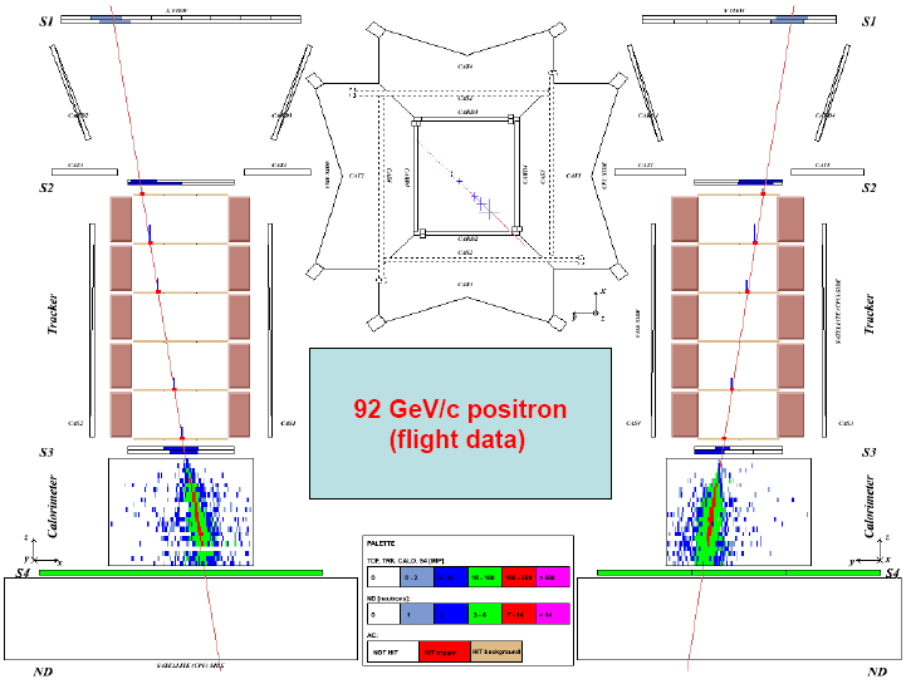

Figure 6. Event display of a 92 GeV/c positron from flight data. Compare the shower topology in the calorimeter with the hadronic shower in figure 5.

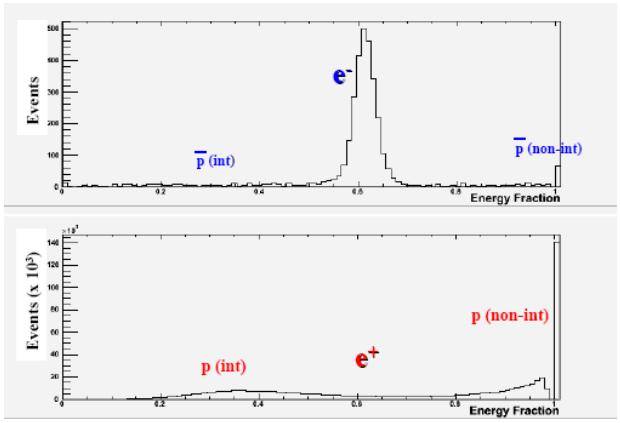

Figure 7. Plot of the energy fraction released along the track in the calorimeter for both negative (top) and positive (bottom) charge in the rigidity interval 20 ÷ 30 GV.

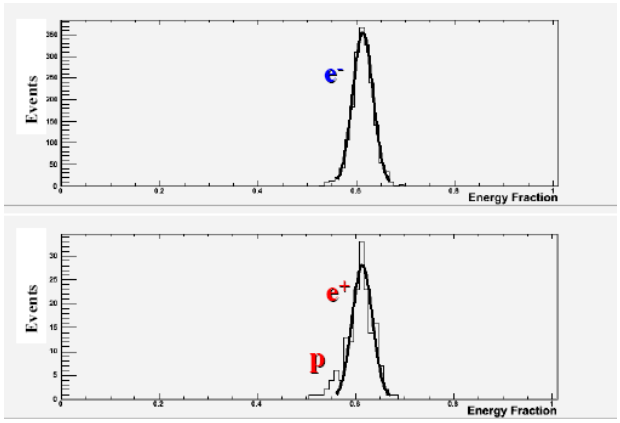

Figure 8. The distributions of figure 7 after applying an energy-momentum match condition and topological cuts related to the shower profile.

References

[1] P. Picozza et al., Astroparticle Physics 27 (2007) 296.
[2] O. Adriani et al., Nucl. Instr. and Meth. A 511 (2003) 72.
[3] G. Osteria et al., Nucl. Instr. and Meth. A 535 (2004) 152.
[4] S. Orsi et al., Adv. Space Res. 37 (2006) 1853.
[5] Y. Stozhkov et al., in: Proc. 19th European Cosmic Ray Symposium, Florence, 2004
Y. Stozhkov et al., Int. J. Modern Phys. A 20 (2004) 6745.
[6] M. Boezio et al., Nucl. Instr. and Meth. A 487 (2002) 407.
[7] V. Bonvicini, "The CR1.4P: an integrated front-end circuit for the imaging calorimeter of PAMELA", in: 5th Intern. Workshop on Front-end Electronics FEE 2003, Snowmass, 2003.